Article

Generation and O Adsorption Studies of the Microporous Magnets CsNi[Cr(CN)] (T = 75 K) and Cr[Cr(CN)]·6HO (T = 219 K)

Steven S. Kaye, Hye Jin Choi, and Jeffrey R. Long

J. Am. Chem. Soc., **2008**, 130 (50), 16921-16925 • DOI: 10.1021/ja803926y • Publication Date (Web): 14 November 2008

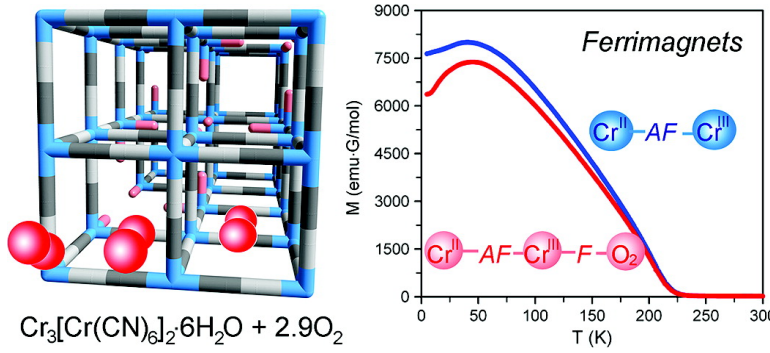

More About This Article

Additional resources and features associated with this article are available within the HTML version:

- Supporting Information
- Access to high resolution figures
- Links to articles and content related to this article
- Copyright permission to reproduce figures and/or text from this article

View the Full Text HTML

J|A|C|S
ARTICLES

Published on Web 11/14/2008

Generation and O_2 Adsorption Studies of the Microporous Magnets $CsNi[Cr(CN)_6]$ (T_C = 75 K) and $Cr_3[Cr(CN)_6]_2 \cdot 6H_2O$ (T_N = 219 K)

Steven S. Kaye, Hye Jin Choi, and Jeffrey R. Long*

Department of Chemistry, University of California, Berkeley, California 94720-1460

Received May 25, 2008; E-mail: jrlong@berkeley.edu

Abstract: Dehydration of the Prussian blue analogues $CsNi[Cr(CN)_6] \cdot 2H_2O$ (**1**) and $Cr_3[Cr(CN)_6]_2 \cdot 10H_2O$ (**2**) affords two new microporous magnets: $CsNi[Cr(CN)_6]$ (**1d**) and $Cr_3[Cr(CN)_6]_2 \cdot 6H_2O$ (**2d**). Compounds **1d** and **2d** maintain the Prussian blue structure, and N_2 adsorption measurements at 77 K show them to be microporous with BET surface areas of 360 and 400 m^2/g, respectively. Both solids largely retain the magnetic properties of their parent hydrates, with **1d** ordering at 75 K and **2d** ordering at 219 K, by far the highest ordering temperature yet observed for a microporous magnet. The compounds further show unexpected changes in their magnetic properties upon adsorption of O_2. In **2d**, adsorption of O_2 results in a reversible decrease in the magnetic moment of the system, as well as a reduction of the coercivity from 110 to 10 G and of the remnant magnetization from 1200 to 400 emu·G/mol, indicating a net antiferromagnetic interaction between O_2 and the framework. In **1d**, adsorption of O_2 instead results in a reversible increase in the magnetic moment of the system, indicating a net ferromagnetic interaction between O_2 and the framework. Together, the results suggest that ferromagnetic exchange coupling between O_2 and the $[Cr(CN)_6]^{3-}$ units provides the predominate magnetic interaction of the adsorbate with the framework.

Introduction

The reduced number of bonds per unit volume associated with a microporous solid is at direct odds with the correlation between the number of exchange pathways and the ordering temperature of a magnet.[1] In addition, the synthesis of a microporous solid that behaves as a magnet at room temperature remains an open challenge. Such compounds are of interest for their potential utility as low-density magnets or magnetic sensors, and possibly even for use in performing magnetic separations, in which the magnetic flux within the pores of the material would selectively attract paramagnetic molecules.[2] Despite the inherent difficulty in producing porous magnetic solids, a variety of such materials have been reported, including metal-organic radical compounds,[3] metal phosphate[4] and sulfate compounds,[5] pillared layer metal hydroxides,[6] metal-organic frameworks,[7] and cyano-bridged coordination solids.[8] For all such materials, the highest ordering temperature yet observed is T_C = 106 K in the cyano-bridged compound $[Mn(HL)]_2Mn[Mo(CN)_7]_2$ (L = *N*,*N*-dimethylalaninol).[8d] Many of these materials exhibit guest dependent changes in the magnetic ordering temperature or other magnetic properties. However, in most cases reported thus far, the guest-dependent properties are due to changes in the metal coordination environment induced by guest adsorption or substitution rather than to magnetic exchange with a paramagnetic adsorbate.

Prussian blue analogues constitute the most extensively investigated class of potentially porous magnetic structures. In these compounds, octahedral $[M'(CN)_6]^{x-}$ complexes are linked via octahedrally coordinated, nitrogen bound M^{y+} ions to give a cubic $M_x[M'(CN)_6]_y$ framework, in which the structure presents $[M'(CN)_6]^{x-}$ vacancies and high water contents with $x > y$ (Figure 1).[9,10] Through appropriate choices of the transition metal ions M and M′, Prussian blue analogues with high magnetic ordering

(1) Larionova, J.; Clérac, R.; Sanchiz, J.; Kahn, O.; Golhen, S.; Ouahab, L. *J. Am. Chem. Soc.* **1998**, *120*, 13088.
(2) Maspoch, D.; Ruiz-Molina, D.; Veciana, J. *Chem. Soc. Rev.* **2007**, 770, and references therein.
(3) (a) Maspoch, D.; Ruiz-Molina, D.; Wurst, K.; Domingo, N.; Cavallini, M.; Biscarini, F.; Tejada, J.; Rovira, C.; Veciana, J. *Nat. Mater.* **2003**, *2*, 190. (b) Maspoch, D.; Domingo, N.; Ruiz-Molina, D.; Wurst, K.; Tejada, J.; Rovira, C.; Veciana, J. *C. R. Chim.* **2005**, *8*, 1213.
(4) (a) Cavellac, M.; Riou, D.; Greneche, J. M.; Férey, G. *J. Magn. Magn. Mater.* **1996**, *163*, 173. (b) Barthelet, K.; Jouve, C.; Riou, D.; Férey, G. *Solid State Sci.* **2000**, *2*, 871. (c) Barthelet, K.; Marrot, J.; Riou, D.; Férey, G. *Angew. Chem., Int. Ed.* **2002**, *41*, 281.
(5) Rujiwatra, A.; Kepert, C. J.; Claridge, J. B.; Rosseinsky, M. J.; Kumagi, H.; Kurmoo, M. *J. Am. Chem. Soc.* **2001**, *123*, 10584.
(6) Kurmoo, M.; Kumagi, H.; Hughes, S. M.; Kepert, C. J. *Inorg. Chem.* **2003**, *42*, 6709.
(7) (a) Guillou, N.; Livage, C.; Drillon, M.; Férey, G. *Angew. Chem., Int. Ed.* **2003**, *42*, 5314. (b) Dybtsev, D. N.; Chun, H.; Yoon, S. H.; Kim, D.; Kim, K. *J. Am. Chem. Soc.* **2004**, *126*, 32. (c) Wang, Z.; Zhang, B.; Fujiwara, H.; Kobayashi, H.; Kurmoo, M. *Chem. Commun.* **2004**, 416. (d) Viertelhaus, M.; Adler, P.; Clérac, R.; Anson, C. E.; Powell, A. K. *Eur. J. Inorg. Chem.* **2005**, 692. (e) Kurumu, M.; Kumagi, H.; Chapman, K. W.; Kepert, C. J. *Chem. Commun.* **2005**, 3012. (f) Kurmoo, M.; Kumagi, H.; Akita-Tanaka, M.; Inoue, K. *Inorg. Chem.* **2006**, *45*, 1627. (g) Cheng, X.; Zhang, W.; Lin, Y.; Zheng, Y.; Chen, X. *Adv. Mater.* **2007**, *19*, 1494. (h) Wang, Z.; Zhang, B.; Zhang, Y.; Kurmoo, M.; Liu, T.; Gao, S.; Kobayashi, H. *Polyhedron* **2007**, *26*, 2207. (i) Huang, Y.-G.; Yuan, D.-Q.; Pan, L.; Jiang, F.-L.; Wu, M.-Y.; Zhang, X.-D.; Wei, W.; Gao, Q.; Lee, J. Y.; Li, J.; Hong, M. C. *Inorg. Chem.* **2007**, *46*, 9609. (j) Navarro, J. A. R.; Barea, E.; Rodriguez-Dieguez, A.; Salas, J. M.; Ania, C. O.; Parra, J. B.; Masciocchi, N.; Galli, S.; Sironi, A. *J. Am. Chem. Soc.* **2008**, *130*, 3978.
(8) (a) Ohkoshi, S.; Arai, K.; Yusuke, A.; Kazuhito, H. *Nat. Mater.* **2004**, *3*, 857. (b) Ohkoshi, S.; Tsunobuchi, Y.; Takahashi, H.; Hozumi, T.; Shiro, M.; Hashimoto, K. *J. Am. Chem. Soc.* **2007**, *129*, 3084. (c) Yanai, N.; Kaneko, W.; Yoneda, K.; Ohba, M.; Kitagawa, S. *J. Am. Chem. Soc.* **2007**, *129*, 3496. (d) Milon, J.; Daniel, M. C.; Kaiba, A.; Guionneau, P.; Brandes, S.; Sutter, J. P. *J. Am. Chem. Soc.* **2007**, *129*, 13872.

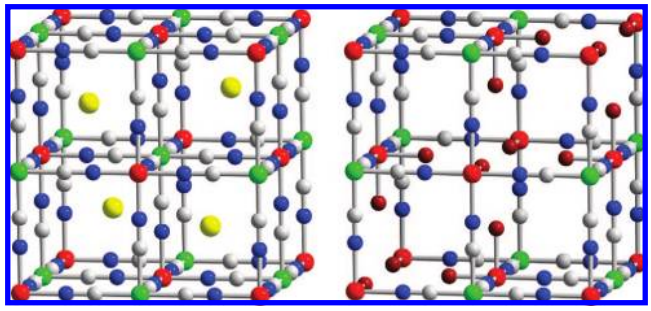

Figure 1. Structures of the Prussian blue analogues, $A^{I}M^{II}[M'^{III}(CN)_6]$ (left) and $M^{II}_3[M'^{III}(CN)_6]_2$ (right) with representative coordinated water molecules shown in dark red. Yellow, red, green, gray, and blue spheres represent A, M, M′, C, and N atoms, respectively. Guest water molecules and hydrogen atoms were omitted for clarity.

temperatures can be constructed.[11] Prominent among these are $CsNi[Cr(CN)_6]\cdot 2H_2O$ (T_C = 90 K),[10] $Cr_3[Cr(CN)_6]_2\cdot 10H_2O$ (T_N = 240 K),[12] $V[Cr(CN)_6]_{0.93}$ (T_N = 315 K),[13] and $KV[Cr(CN)_6]_2$ (T_N = 376 K).[14] Prussian blue analogues have also shown the potential for high surface area, with dehydrated compounds of the type $M_3[Co(CN)_6]_2$,[15] $M_3[Fe(CN)_6]_2$,[16] and $M[Fe(CN)_5(NO)]$[17] exhibiting BET surface areas ranging from 520 to 870 m^2/g. To date, however, the only Prussian blue analogues in which microporosity and bulk magnetic ordering have been demonstrated to coexist are $M_3[Fe(CN)_6]_2$ (T_C = 10 K for M = Mn, 14 K for M = Co, 25 K for M = Ni, and 22 K for M = Cu),[16] $Co_3[Co(CN)_5]_2$ (T_N = 38 K),[18] and $K_{0.2}Mn_{1.4}[Cr(CN)_6]$ (T_N = 99 K).[19]

Herein, we report desolvation of the Prussian blue analogues $CsNi[Cr(CN)_6]\cdot 2H_2O$ (**1**) and $Cr_3[Cr(CN)_6]_2\cdot 10H_2O$ (**2**) to give $CsNi[Cr(CN)_6]$ (**1d**) and $Cr_3[Cr(CN)_6]_2\cdot 6H_2O$ (**2d**), microporous magnets with BET surface areas of 360 and 400 m^2/g and magnetic ordering temperatures of 75 and 219 K, respectively. Unexpectedly, both materials were found to exhibit changes in their magnetic properties upon adsorption of O_2 but not N_2, indicating the presence of magnetic exchange coupling between the O_2 guest molecules and the frameworks.

Experimental Section

Preparation of Compounds. Reactions involving Cr^{2+} salts were performed inside a glovebag under a nitrogen atmosphere. The compound $K_3[Cr(CN)_6]$ was prepared according to a previously reported procedure.[20] Water was distilled and deionized with a Milli-Q filtering system and was subsequently degassed by rapidly stirring under reduced pressure (ca. 10^{-3} bar) for 4 h. All other reagents were obtained from commercial vendors and, unless otherwise noted, were used without further purification.

$CsNi[Cr(CN)_6]\cdot 2H_2O$ (1). The synthesis of this compound was based upon a modification of a previously reported procedure.[10] A solution of $NiCl_2$ (240 mg, 1.0 mmol) in 30 mL of H_2O was added dropwise to a stirred solution of $K_3[Cr(CN)_6]$ (330 mg, 1.0 mmol) and CsCl (340 mg, 2.0 mmol) in 10 mL of water. The resulting light blue precipitate was allowed to anneal in the mother liquor for 1 h and was then collected by filtration and washed with successive aliquots of water (3 × 30 mL). The solid was dried under reduced pressure to afford 400 mg (92%) of product as a yellow microcrystalline powder. Anal. Calcd for $C_6H_4CrCsN_6NiO_2$: C, 16.54; H, 0.93; Cr, 11.93; N, 19.29; Ni, 13.47. Found: C, 16.85; H, 1.17; Cr, 11.99; N, 19.57; Ni, 13.24. Elemental analysis further indicated the presence of less than 0.05 equiv of K. The powder X-ray diffraction pattern of this compound agrees with that of a typical Prussian blue type solid exhibiting a face-centered cubic unit cell.

$CsNi[Cr(CN)_6]$ (1d). A sample of **1** (100 mg, 0.75 mmol) was heated to 95 °C under reduced pressure (ca. 10^{-7} bar) for 48 h to give the product as a yellow microcrystalline solid in quantitative yield. Anal. Calcd for C_6CrCsN_6Ni: C, 18.03; Cr, 13.01; N, 21.02; Ni, 14.68. Found: C, 18.24; Cr, 12.87; N, 21.24; Ni, 14.79. Elemental analysis further indicated the presence of less than 0.05 equiv of K. The powder X-ray diffraction pattern of this compound agrees with that of a typical Prussian blue type solid exhibiting a face-centered cubic unit cell.

$Cr_3[Cr(CN)_6]_2\cdot 10H_2O$ (2). The synthesis of this compound was based upon a modification of a previously reported procedure.[12] A solution of $CrCl_2$ (370 mg, 3.0 mmol) in 10 mL of water was filtered through a plug of Celite to remove insoluble impurities. A solution of $K_3[Cr(CN)_6]$ (330 mg, 1.0 mmol) in 10 mL of water was then added dropwise to the purified $CrCl_2$ solution under vigorous stirring. The resulting gray precipitate was allowed to anneal in the mother liquor for 12 h and was then collected by filtration and washed with successive aliquots of water (3 × 30 mL). The solid was dried in air to afford 360 mg (96%) of product as a gray microcrystalline powder. Anal. Calcd for $C_{12}H_{20}Cr_5N_{12}O_{10}$: C, 19.16; H, 2.68; Cr, 34.6; N, 22.34. Found: C, 19.47; H, 2.55; Cr, 34.1; N, 22.20. Elemental analysis further indicated the presence of less than 0.05 equiv of K. The powder X-ray diffraction pattern of this compound agrees with that of a typical Prussian blue type solid exhibiting a face-centered cubic unit cell.

$Cr_3[Cr(CN)_6]_2\cdot 6H_2O$ (2d). A sample of **2** (100 mg, 0.13 mmol) was heated to 85 °C under reduced pressure (ca. 10^{-7} bar) for 48 h to give the product as a gray microcrystalline solid in quantitative yield. Anal. Calcd for $C_{12}H_{12}Cr_5N_{12}O_6$: C, 21.19; H, 1.78; Cr, 38.22; N, 24.71. Found: C, 21.36; H, 1.63; Cr, 38.12; N, 24.60. Elemental analysis further indicated the presence of less than 0.05 equiv of K. The powder X-ray diffraction pattern of this compound agrees with that of a typical Prussian blue type solid exhibiting a face-centered cubic unit cell.

Gas Adsorption Measurements. Sample tubes of a known weight were loaded with 100−300 mg of sample and sealed using a transeal. Samples were degassed at 85 or 95 °C for 24−48 h on a Micromeritics ASAP 2020 analyzer until the outgas rate was less than 1 mTorr/min. The degassed sample and sample tube were weighed precisely and then transferred back to the analyzer (with the transeal preventing exposure of the sample to air after degassing). The outgas rate was again confirmed to be less than 1 mTorr/min. Samples were maintained at constant temperature by immersion in baths of liquid nitrogen (77 K), liquid argon (87 K), ethanol/liquid nitrogen (157 K), heptane/liquid nitrogen (182 K), acetone/dry ice (195 K), octane/liquid nitrogen (217 K), or acetonitrile/liquid nitrogen (232 K). UHP grade N_2, O_2, and He (99.999%) gases were used for all measurements.

(9) Buser, H. J.; Schwarzenbach, D.; Petter, W.; Ludi, A. *Inorg. Chem.* **1977**, *16*, 2704.
(10) Gadet, V.; Mallah, T.; Castro, I.; Verdaguer, M.; Veillet, P. *J. Am. Chem. Soc.* **1992**, *114*, 9213.
(11) Verdaguer, M.; Bleuzen, A.; Marvaud, V.; Vaissermann, J.; Seuleiman, M.; Desplanches, C.; Scuiller, A.; Train, C.; Garde, R.; Gelly, G.; Lomenech, C.; Rosenman, I.; Veillet, P.; Cartier, C.; Villain, F. *Coord. Chem. Rev.* **1999**, *190−192*, 1023, and references therein.
(12) Mallah, T.; Thiebaut, S.; Verdaguer, M.; Veillet, P. *Science* **1993**, *262*, 1554.
(13) (a) Ferlay, S.; Mallah, T.; Ouhes, R.; Veillet, P.; Verdaguer, M. *Nature* **1995**, *378*, 701. (b) Hatlevik, O.; Buschmann, W. E.; Zhang, J.; Manson, J. L.; Miller, J. S. *Adv. Mater.* **1999**, *11*, 914.
(14) Holmes, S. M.; Girolami, G. S. *J. Am. Chem. Soc.* **1999**, *121*, 5593.
(15) (a) Kaye, S. S.; Long, J. R. *J. Am. Chem. Soc.* **2005**, *127*, 6506. (b) Chapman, K. W.; Southon, P. D.; Weeks, C. L.; Kepert, C. J. *Chem. Commun.* **2005**, 3322.
(16) Martinez-Garcia, R.; Knobel, M.; Reguera, E. *J. Phys.: Condens. Matter* **2006**, *18*, 11243.
(17) Culp, J. T.; Matranga, C.; Smith, M.; Bittner, E. W.; Bockrath, B. *J. Phys. Chem. B* **2006**, *110*, 8325.
(18) (a) Beauvais, L. G.; Long, J. R. *J. Am. Chem. Soc.* **2002**, *124*, 12096. (b) Kaye, S. S.; Long, J. R. *Catal. Today* **2007**, *120*, 311.
(19) Lu, Z.; Wang, X.; Liu, Z.; Liao, F.; Gao, S.; Xiong, R.; Ma, H.; Zhang, D.; Zhu, D. *Inorg. Chem.* **2006**, *45*, 999.
(20) Marvaud, V.; Mallah, T.; Verdaguer, M.; Biner, M.; Decurtins, S. *Inorg. Synth.* **2004**, *34*, 144.

Enthalpies of adsorption were calculated by fitting the data to the van't Hoff equation:[21]

$$\ln(P) = \frac{\Delta H_{ads}}{RT} + \frac{\Delta S_{ads}}{R} \quad (1)$$

where P is the pressure, T is the temperature, R is the molar gas constant, ΔH_{ads} is enthalpy of adsorption, and ΔS_{ads} is the entropy of adsorption. This equation can be used to calculate the enthalpy of adsorption as a function of the quantity of gas adsorbed. Pressure as a function of the quantity of gas adsorbed was calculated by fitting each isotherm using the Langmuir−Freundlich equation:[21]

$$\frac{Q}{Q_m} = \frac{B \cdot P^{1/t}}{1 + B \cdot P^{1/t}} \quad (2)$$

where Q is the number of moles of gas adsorbed, Q_m is the number of moles of gas adsorbed at saturation, P is the pressure, and B and t are fitting constants. In order to obtain the most accurate interpolation between measured data points, fits were only applied to regions of the isotherm that were used to calculate the enthalpy of adsorption. Similar results were obtained when virial equations were employed in fitting the isotherms.[22]

Magnetic Susceptibility Measurements. Quartz sample tubes were loaded with 15−30 mg of sample and degassed under reduced pressure (10^{-7} bar) at 85 or 95 °C for 48 h. The tubes were then flame-sealed, and the magnetic susceptibility measurements were performed using a Quantum Design MPMS2 SQUID magnetometer. For samples measured in the presence of adsorbed gas, prior to sealing the sample tube, the degassed samples were cooled to 77 K and the sample tubes pressurized to 50 Torr with dioxygen or dinitrogen for 10 min. The amount of gas adsorbed by the sample was calculated using the gas adsorption measurements described above.

Other Physical Measurements. Elemental analyses for C, H, and N were obtained from the Microanalytical Laboratory of the University of California, Berkeley, and analyses for K, Cr, and Ni were obtained from Huffman Laboratories. Thermogravimetric analyses were carried out at a ramp rate of 0.5 °C/min using a TA Instruments Q5000 analyzer. Powder X-ray diffraction data were collected using Cu Kα (λ = 1.5406 Å) radiation on a Siemens D5000 diffractometer.

Results and Discussion

For these investigations, we focused on the compounds $CsNi[Cr(CN)_6] \cdot 2H_2O$ (**1**) and $Cr_3[Cr(CN)_6]_2 \cdot 10H_2O$ (**2**), which are the two highest-ordering, crystalline Prussian blue analogues that are not antiferromagnets. Samples were prepared using modifications of previously reported procedures, as described above.[10,12] The X-ray powder diffraction patterns of both products were fully consistent with the usual Prussian blue structure type, but showed broadened peaks, suggesting very small crystallite sizes. Elemental analyses confirmed the composition of both compounds and indicated the presence of less than 0.05 equiv of potassium per formula unit. Compounds **1** and **2** were dehydrated by heating under reduced pressure (10^{-7} bar) for 48 h at 85 and 95 °C, respectively, to give $CsNi[Cr(CN)_6]$ (**1d**) and $Cr_3[Cr(CN)_6]_2 \cdot 6H_2O$ (**2d**). In **2d**, the six remaining water molecules are likely coordinated to the Cr^{2+} ions. Attempts to completely dehydrate **2** by heating at higher temperatures resulted in amorphous materials that exhibited no magnetic ordering at temperatures down to 5 K.

The porosity of the dehydrated samples was probed via N_2 adsorption measurements performed at 77 K. As shown in Figure 2, isotherms for both materials showed a steep initial rise below

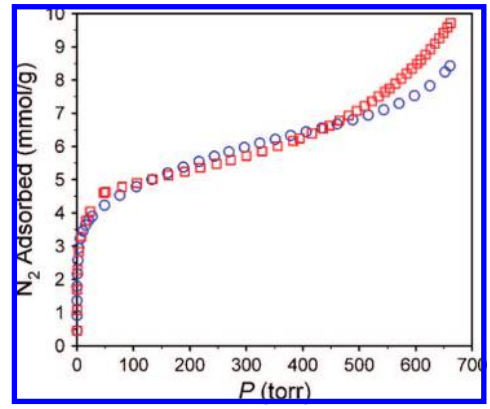

Figure 2. Nitrogen adsorption isotherms for **1d** (red squares) and **2d** (blue circles), as measured at 77 K.

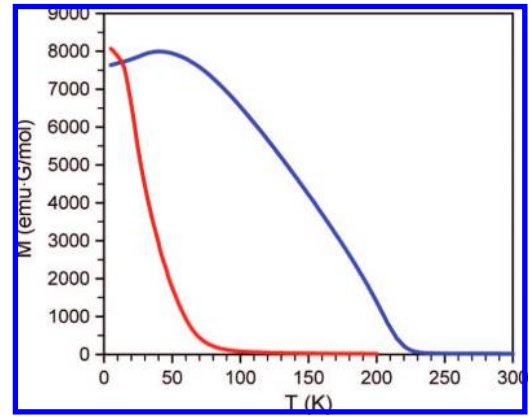

Figure 3. Field-cooled magnetization data for **1d** (red) and **2d** (blue), as measured in an applied field of 1000 Oe.

50 Torr due to adsorption in the internal micropores, followed by a gradual increase from 50−660 Torr, likely due to adsorption on the surface of the particles. Fits of the data to the BET equation gave surface areas of 360 and 400 m^2/g for **1d** and **2d**, respectively. The lower surface areas of these materials relative to the 520−870 m^2/g reported for a variety of other Prussian blue analogues[15−18] are presumably due to the partial occupancy of the pores by Cs^+ ions in the case of **1d** and H_2O in the case of **2d**, together with the lack of cyanometallate vacancies in the former case.

Remarkably, the magnetic properties of **1** and **2** are largely retained by the dehydrated materials. As shown in Figure 3, magnetization data for **1d** indicate a ferromagnet with an ordering temperature of T_C = 75 K, compared with T_C = 90 K for **1**.[10] The room temperature magnetic susceptibility for **1d** gives $\chi_M T$ = 3.32 emu K/mol, similar to the value of 2.88 emu K/mol expected for one Ni^{2+} (S = 1) ion and one Cr^{3+} (S = ³⁄₂) ion per formula unit, assuming no exchange coupling and g = 2.00. The moment of **1d** continuously rises with decreasing temperature, and a fit of the data to the Curie−Weiss law gives a positive Weiss constant of θ = 74 K (see Figure S1 in the Supporting Information), indicating the expected ferromagnetic coupling between Ni^{2+} and Cr^{3+} ions. No significant magnetic hysteresis is observed for **1d** at temperatures down to 2 K, which is in accordance with the very small coercivity (H_c = 70 Oe) observed for the parent compound **1**.[10] As the magnetic coercivity can also be reduced by smaller grain size, even if Ni^{2+} has been known to possess significant single-ion anisotropy, compound **1d** is likely

(21) Roquerol, F.; Rouquerol J.; Sing, K. *Adsorption by Powders and Solids: Principles, Methodology, and Applications*; Academic Press: London, 1999.
(22) Do, D. D. *Adsorption Analysis: Equilibria and Kinetics*; Imperial College Press: London, 1998.

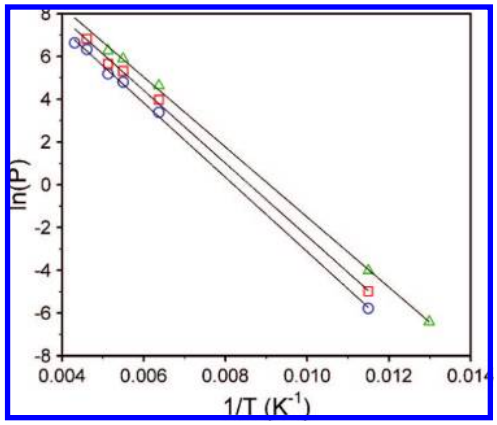

Figure 4. van't Hoff isosteres for O_2 adsorption in **2d**. Blue circles, red squares, and green triangles correspond to adsorption of 0.25, 0.35, and 0.50 mmol O_2/g. Solid lines represent the best linear fits to the data.

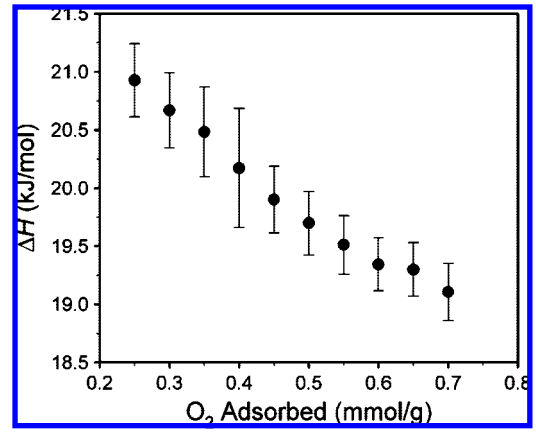

Figure 5. Enthalpy of O_2 adsorption for **2d**. Error bars represent one standard deviation.

to lose anisotropy due to the very small crystallite sizes as well as the high symmetry of the Prussian blue structure type.[23]

The magnetization data for **2d**, also shown in Figure 3, are indicative of a ferrimagnet with an ordering temperature of T_N = 219 K, nearly identical to the value of T_N = 220 K observed for **2**.[24] This represents the highest ordering temperature yet reported for a microporous magnet. The room temperature magnetic susceptibility for **2d** gives $\chi_M T$ = 5.64 emu K/mol, somewhat lower than the value of 12.75 emu K/mol expected for two high-spin Cr^{2+} (S = 2) ions and three Cr^{3+} (S = 3/2) ions per formula unit, assuming no exchange coupling and g = 2.00, due to the antiferromagnetic coupling at room temperature.[12] As the sample is cooled, the moment decreases and reaches a minimum at 287 K. This, together with the negative Weiss constant of $\theta = -570$ K, obtained using Neel's hyperbolic equation[25] (see Figure S2 in the Supporting Information), indicates antiferromagnetic coupling between adjacent metal centers. Consistent with ferrimagnetism, magnetic hysteresis is observed at 5 K, with a loop characterized by a coercive field of 110 Oe and a remnant magnetization of 1200 emu·G/mol, comparable to the values of 20 Oe and 1333 emu·G/mol observed for **2**.[12]

To investigate the effect of the magnetic field of a porous magnet on a paramagnetic adsorbent, O_2 adsorption isotherms were measured for **2d** at temperatures ranging from 77 to 232 K (see Figure S3 in the Supporting Information). For a gas adsorbing on a diamagnetic material, the enthalpy and entropy of adsorption are typically constant as a function of temperature.[21] According to the van't Hoff equation (see eq 1), a plot of ln(P) versus T^{-1} should therefore be linear. In contrast, for a paramagnetic gas adsorbing on a ferrimagnetic material, the enthalpy of adsorption is augmented by the enthalpy associated with the alignment of the magnetic moment of the gas molecules with the magnetic field within the pores of the material. Since the strength of this interaction increases with decreasing temperature, the slope of ln(P) versus T^{-1} should increase as the temperature increases. The van't Hoff plots constructed from the O_2 adsorption isotherms for **2d** are depicted in Figure 4. Importantly, the plots show no significant deviation from linearity, with fits to the isosteres having R^2 values between 0.994 and 0.999. The coverage dependent enthalpy of adsorption calculated from these isosteres is shown in Figure 5 and ranges from 20.9 to 19.1 kJ/mol. The standard deviation in the enthalpy is less than 0.5 kJ/mol over the measured range, indicating that any magnetic interaction between O_2 and the framework must be very weak. Thus, the possibility of utilizing the microporous magnet **2d** for the efficient separation of O_2 from air looks to be unrealizable. For **1d**, which has a much lower ordering temperature than **2d**, we do not expect significant interaction of O_2 with the internal magnetic field of the solid at such temperatures. Here, O_2 adsorption isotherms were measured at 77 and 87 K, revealing an enthalpy of O_2 adsorption of 12.0 kJ/mol, which is nearly half of that of **2d** (Figure S6 in the Supporting Information). This effect is likely associated with the structural differences between the two compounds (see Figure 1), which give rise to significantly different pore environments.

In an attempt to better characterize the weak interactions between adsorbed O_2 molecules and the cyano-bridged framework, the magnetic properties of **1d** and **2d** were studied in the presence of an atmosphere of O_2. In **2d**, the presence of 2.9 molecules of O_2 per formula unit, nearly all of which should be adsorbed at 77 K, causes a decrease in the magnetic moment of the system, as well as a reduction in the coercivity from 110 to 10 Oe and the remnant magnetization from 1200 to 440 emu·G/mol (see Figure 6). Both the decrease in the magnetic moment and coercivity are fully reversible upon desorption of O_2. Furthermore, no changes in the magnetic properties of **2d** are observed upon adsorption of the diamagnetic gas N_2, suggesting that the O_2 molecules are actually coupling with the framework, rather than simply inducing a change in the structure of **2d**. To our knowledge, this is the first report of magnetic exchange between a microporous magnet and a paramagnetic adsorbate. At higher magnetic field, the magnetization for **2d**-O_2 does not saturate, but linearly increases up to M = 2.12 $N\beta$ at 60 G.[26] This linear increase has been observed previously for adsorbed O_2 molecules on a diamagnetic porous solid,[27a] where magnetic interaction between the aligned O_2 molecules resulted in linear magnetization up to 5 T at temperatures below 60 K. Also, the magnetic study on the frozen bulk O_2 phase has revealed a

(23) (a) Entley, W. R.; Girolami, G. S. *Science* **1995**, *268*, 397. (b) Entley, W. R.; Girolami, G. S. *Inorg. Chem.* **1994**, *33*, 5165. (c) Stump, H. O.; Pei, Y.; Michaut, C.; Kahn, O.; Renard, J. P.; Ouahab, L. *Chem. Mater.* **1994**, *6*, 257.

(24) In our hands, compound **2** exhibited ordering temperature of T_N = 220 K, as estimated by a fit of the susceptibility data to Neél's hyperbolic equation. This is somewhat lower than the value of T_N = 240 K reported in ref 12.

(25) Smart, J. S. *Am. J. Phys.* **1955**, *23*, 356.

(26) In our measurement, the saturation was far from being complete, as consistently observed for the parent compound $Cr_3[Cr_2(CN)_6]\cdot 10H_2O$ in ref 12, where the maximum magnetization observed was 1.4 $N\beta$ at 10 K and 70 kOe.

(27) (a) Takamizawa, S.; Nakata, E.; Akatsuka, T. *Angew. Chem., Int. Ed.* **2006**, *45*, 2216. (b) Uyeda, C.; Sugiyama, K.; Date, M. *J. Phys. Soc. Jpn.* **1985**, *54*, 1107.

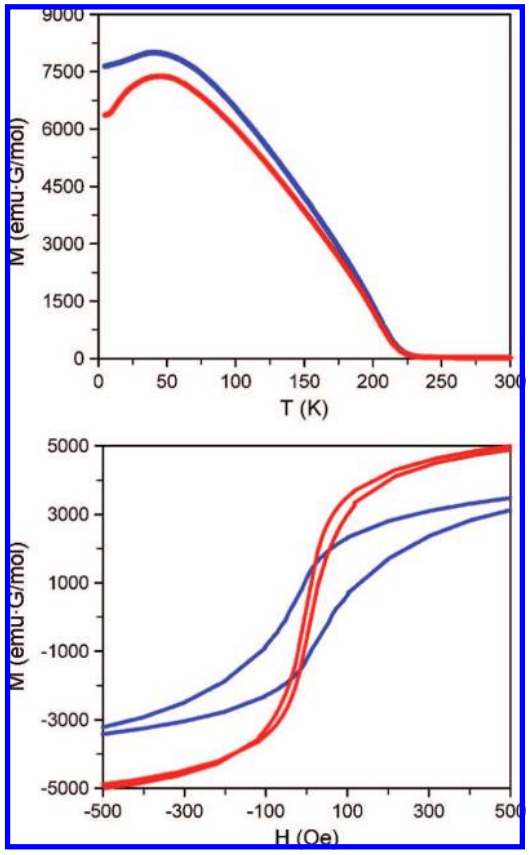

Figure 6. Magnetic behavior of **2d** (blue) and **2d** sealed in a quartz tube containing 2.9 molecules of O_2 per formula unit (red). Top: Field-cooled magnetization data, as measured in an applied field of 1000 Oe. Bottom: Magnetic hysteresis loops, as measured at 5 K.

linear increase in magnetization upon the increasing magnetic field up to 50 T.[27b] Therefore, among the 2.9 molecules O_2 per formula unit in **2d**-O_2, some portion is apparently not participating in the magnetic coupling with the framework due to the small pore size but has magnetic interaction between themselves. The complexity of the integrated magnetic interactions including those between O_2 molecules, O_2 and the framework, and Cr^{2+} and Cr^{3+} in the framework hampered the quantitative analysis of the spin magnetization. Indeed, consistent with our observations for **2d**, the magnetization of the parent compound **2** also does not saturate under the conditions probed.[12]

A somewhat larger effect is observed for O_2 adsorbed within **1d**. Here, adsorption of 1.8 molecules of O_2 per formula unit causes an *increase* in the moment of the system, as shown in Figure 7. As with the **2d**-O_2 system, this change in the magnetic properties is fully reversible upon desorption of O_2, and no effect is observed upon adsorption of N_2, indicating that O_2 is coupling ferromagnetically with the framework. Although the specifics of the exchange mechanism are unclear, we note that the switch from a net antiferromagnetic effect in **2d**-O_2 to ferromagnetic coupling in **1d**-O_2 is at least consistent with the predominate interaction being ferromagnetic exchange between O_2 and the $[Cr(CN)_6]^{3-}$ units of the frameworks. At 2 K, no significant difference in hysteresis was observed between **1d** and **1d**-O_2, other than the change in magnetization values (see Figure 7). Similar to the situation with **2d**-O_2, the field-dependent magnetization in **1d**-O_2 is highly increasing without saturation due to the combination of the ferromagnetic interaction between **1d** and O_2, and the magnetization increase of O_2, thus preventing a quantitative spin analysis.

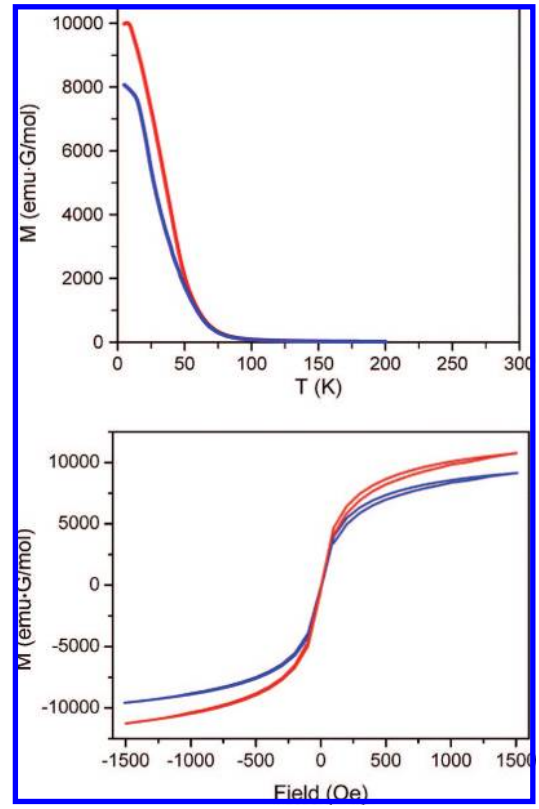

Figure 7. Magnetic behavior of **1d** (blue) and **1d** sealed in a quartz tube containing 1.8 molecules of O_2 per formula unit (red). Top: Field-cooled magnetization data, as measured in an applied field of 1000 Oe. Bottom: Magnetic hysteresis loops, as measured at 2 K.

The foregoing results show that microporous magnets with high ordering temperatures can be generated by dehydrating Prussian blue analogues already known to exhibit strong magnetic exchange. Although the magnetic flux within the pores of **2d** is insufficient to cause a significant deviation from van't Hoff behavior, the adsorption of O_2 does result in a net antiferromagnetic interaction with the ferrimagnetic framework. Interestingly, this exhange interaction switches to ferromagnetic for O_2 adsorbed within the ferromagnet **1d**, suggesting that ferromagnetic coupling between O_2 and the $[Cr(CN)_6]^{3-}$ units provides the predominate exchange pathway in each material. Future work will include powder X-ray diffraction measurements to identify the O_2 binding sites within these structures, which may lend additional insight into the origin of the magnetic coupling. In addition, attempts will be made to further increase the ordering temperatures and pore flux density within microporous magnets, through, for example, the incorporation of species such as $[Mo(CN)_6]^{3-}$ into Prussian blue analogues.[28,29]

Acknowledgment. This research was funded by DoE Grant No. DE-FG03-01ER15257. We thank the National Science Foundation for providing S.S.K. with a predoctoral fellowship, and Prof. S. Kitagawa for helpful discussions.

Supporting Information Available: Additional plots of adsorption isotherms and magnetic data. This material is available free of charge via the Internet at http://pubs.acs.org.

JA803926Y

(28) Beauvais, L. G.; Long, J. R. *J. Am. Chem. Soc.* **2002**, *124*, 2110.
(29) Ruiz, E.; Rodriguez-Fortea, A.; Alvarez, S.; Verdaguer, M. *Chem.—Eur. J.* **2005**, *11*, 2135.